

# Remotely sensed desertification modeling using ensemble of machine learning algorithms

Abdolhossein Boali<sup>a</sup>, Hamid Reza Asgari<sup>b,\*</sup>, Ali Mohammadian Behbahani<sup>c</sup>, Abdolrassoul Salmanmahiny<sup>d</sup>, Babak Naimi<sup>e</sup>

<sup>a</sup> Department of Arid Zone Management, Gorgan University of Agricultural Sciences and Natural Resources, Gorgan, Golestan, Iran

<sup>b</sup> Department of Arid Zone Management, Gorgan University of Agricultural Sciences and Natural Resources, Gorgan, Golestan, Iran

<sup>c</sup> Department of Watershed and Arid Zone Management, Gorgan University of Agricultural Sciences and Natural Resources, Gorgan, Golestan, Iran

<sup>d</sup> Department of Environmental Sciences, Gorgan University of Agricultural Sciences and Natural Resources, Gorgan, Golestan, Iran

<sup>e</sup> Department of Biology, University of Utrecht, Padualaan 8, Utrecht, 3584 CH, The Netherlands

## ARTICLE INFO

### Keywords:

Modeling  
Machine learning methods  
Desertification maps  
Remote sensing  
MEDALUS

## ABSTRACT

Due to having a sensitive and fragile ecosystem, dry areas are constantly exposed to land degradation and desertification. Therefore, it is necessary to formulate appropriate strategies for quantitative assessment of desertification that are highly accurate. In this research, desertification of the region was first evaluated using MEDALUS model, then according to the results of MEDALUS model and reviewing the results of other researchers, 8 indicators remote sensing that had the highest correlation with field data were selected for modeling. Four machine learning methods Support Vector Machine (SVM), Gradient Boosting Machine (GBM), Generalized Linear Models (GLM) and Random Forests (RF) were used to model the risk of desertification in northeastern Iran. Finally, the weighted average of the ensemble model in the SDM statistical package was used to predict the desertification of the region. Based on the results obtained from MEDALUS model, the indicators of drought resistance (score 162), conservation operations (score 158) and soil salinity (score 155), in the working units of abandoned lands, wetland lands, and Salty lands located in the north East of the region, have increased the process of desertification. The results of modeling using machine learning methods showed that in 2002, the SVM model (AUC = 0.91, TSS = 0.93, and Kappa = 0.86) and in 2021, the RF model (AUC = 0.94, TSS = 0.94, and Kappa = 0.90) have performed best. The forecast of the combined model for desertification in 2021 in the studied area showed that the northeastern and sporadically in the central parts of the studied area are affected by the progress of the desertification process. Therefore, by considering the results of the combined model (as a model with the least uncertainty), it is possible to reduce the progress of the desertification process by planning, optimal management and applying corrective methods in the areas affected by desertification.

## 1. Introduction

Arid regions around the world are highly susceptible to environmental changes that can result in land degradation and

\* Corresponding author.

E-mail addresses: [Hossien.boali@yahoo.com](mailto:Hossien.boali@yahoo.com) (A. Boali), [hamidreza.asgari@gau.ac.ir](mailto:hamidreza.asgari@gau.ac.ir) (H.R. Asgari), [ali.mohammadian@gau.ac.ir](mailto:ali.mohammadian@gau.ac.ir) (A. Mohammadian Behbahani), [mahini@gau.ac.ir](mailto:mahini@gau.ac.ir) (A. Salmanmahiny), [naimi.b@gmail.com](mailto:naimi.b@gmail.com) (B. Naimi).

<https://doi.org/10.1016/j.rsase.2024.101149>

Received 15 May 2023; Received in revised form 10 January 2024; Accepted 26 January 2024

Available online 13 February 2024

2352-9385/© 2024 Elsevier B.V. All rights reserved.

desertification (Prävalie, 2021; United Nations, 1994). This phenomenon can be the consequence of multiple interacting factors including climate change and anthropogenic effects such as agricultural and industrial activities (Zeng et al., 2021). Desertification is a significant global concern, causing an annual economic loss of 42 billion US dollars and affecting two billion people directly or indirectly, with five million people being forced to migrate each year (Elnashar et al., 2022). This issue is particularly important for countries facing droughts, especially those in arid and semi-arid regions that are highly vulnerable to desertification. In recent decades, the combination of climate change and human activities has accelerated desertification rates in many of these countries.

In order to combat desertification, mitigate its adverse effects, and prevent its spread (Duan et al., 2019), effective solutions are required to identify areas prone to desertification, assess land degradations, and monitoring their status. One way to address this problem is through modeling, which allows for the analysis, prediction, and investigation of environmental events associated with desertification (Meng et al., 2021). Although desertification modeling presents a promising approach for understanding the mechanisms leading to land degradation and desertification and addressing their associated complex challenges (Elnashar et al., 2022), it is not without limitations. One key challenge is the difficulty of obtaining accurate and comprehensive data on the environmental factors that contribute to desertification. Traditionally, modeling and monitoring methods relied heavily on expensive and time-consuming field observations (Wen et al., 2020). However, recent advances in remote sensing and machine learning have provided new opportunities to improve the efficiency and accuracy of desertification modeling. By leveraging the power of these tools, researchers can quickly and accurately gather data on key environmental factors, such as changes in land use, vegetation cover, and soil moisture, and use this information to develop more effective strategies for mitigating and preventing desertification. The use of remote sensing and machine learning approaches also has the potential to provide policymakers and land managers with critical insights into the long-term impacts of different land management practices, allowing them to make more informed decisions about how best to allocate resources and manage their land sustainably. Ultimately, the integration of remote sensing and machine learning into desertification modeling represents a significant step forward in our collective efforts to combat this pressing environmental challenge.

Given the importance of desertification as a global environmental issue, numerous studies have been conducted to address this challenge. Several models have been developed to generate desertification maps at the regional scale, including Food and Agriculture Organization of the United Nations (FAO-UNEP), Iranian Classification of Desertification (ICD) and Mediterranean and Land Use Sensitive (MEDALUS) (Akbari et al., 2016). Among these models, MEDALUS, developed by the European Commission, has been recognized as one of the best methods to assess desertification and used widely in various Mediterranean and Middle Eastern countries (Budak et al., 2018; Ferrara et al., 2020; Afzali et al., 2021; Bouhata and Bensekhria, 2021). However, the main challenge in using this model is the extensive spatial and temporal data required (Elnashar et al., 2022), which is difficult to obtain using field survey alone. Moreover, as desertification mainly occurs in arid regions, the extraction of large-scale information in the long term is challenging (Duan et al., 2019). To overcome these limitations, remote sensing can play an essential role for data collection, enabling to the evaluation, monitoring and modeling of desertification status, and identification of the underlying causes of desertification development (Jiang et al., 2019; Meng et al., 2021). This approach has been shown to provide more efficient and accurate data than field surveys, particularly for large-scale assessment and predictions (Abuzaid and Abdelatif, 2022).

Desertification monitoring is typically conducted using either single-index or multi-index methods (Meng et al., 2021). Single-index methods usually rely on single indicator methods, such as applying a threshold on a Normalized difference vegetation index (NDVI), to classify the extent of desertification (Filei et al., 2018; Bezerra et al., 2020). However, this approach ignores other important indicators, leading to decreased accuracy in classification results (Wei et al., 2018). While single-index methods are simple and cost-effective, they provide less information about environmental changes compared to multi-indicator methods, which are more accurate and provide more comprehensive information. In this study, we will use machine learning that enables utilizing a multi-indicator method for desert modeling and forecasting, taking into account indices such as NDVI, albedo, surface soil grain size index (TGSI), and land surface temperature (Duan et al., 2019; Guo et al., 2020; Wei et al., 2020). By considering multiple indicators, we expect to obtain more accurate results. The most commonly used machine learning methods for desertification monitoring are decision trees and random forests (RF) methods (Lamchin et al., 2016; Duan et al., 2019). However, using a single method alone may not provide the most accurate results, and weaker models can be combined to produce better results. Therefore, in this study, we will use a coupled machine learning model from the SDM package in R (Naimi and Araújo, 2016) to generate more realistic classifications.

The objective of this study is to utilize an ensemble of machine learning models, trained on remotely sensed data, to assess desertification and predict its spatial distribution. We implemented our study in a region, Northeastern Iran which is located in the Southeast of the Caspian Sea and in the Southwest of the Qaraqum desert of Turkmenistan. The region's unique climatic and ecological conditions have resulted in to land degradation through processes such as water and wind erosion, land use change, and groundwater depletion, indicating progressive desertification. In this investigation, we first employed the MEDALUS model to evaluate the desertification process in the region. We then converted the key impact indicators identified by the MEDALUS model into RS indicators and built machine learning models that can predict or project desertification over different time ranges based on these indicators. Finally, we present a comprehensive remote sensing-based model that can evaluate desertification from multiple aspects, and has the ability to monitor and predict desertification at both local and regional scales.

## 2. Materials and methods

### 2.1. Study area

The study was conducted in the Northeastern region of Iran, specifically in the Northwest of Golestan province. The area spans over 3094 km<sup>2</sup> and is bordered by desert lands and Turkmenistan in the North, Caspian Sea coastal plains to the west, Gorgan city to the South (the capital city of Golestan province), and Gonbad city to the East (Fig. 1). The area has varying altitude, with the highest and

lowest points located in the southern and western parts, respectively. The region is mostly used for pasture and is covered by marine, flood and wind sediments. The climate of the area is classified as dry and cold based on de Marton (1926) and Ivanov (1941) methods, with an average annual rainfall, evaporation and temperature of 464 mm, 1338 mm and 18.17 °C, respectively during the 30-year period (1991–2021). The study utilized the topographic and geological maps, field visits, and aerial image interpretation to identify different geomorphological facies in the area, with each facies serving as a working unit. In total, 13 work units were identified to assess desertification in the region (see Fig. 2).

## 2.2. Field studies

In July 2021, 42 soil characteristics such as salinity, texture, and drainage indices were measured using 42 soil samples collected from the study area. Vegetation evaluation was conducted by establishing one square meter plot along a 100 m transect, with three transects in each work unit and 10 plots in each transect. The percentage of vegetation in each plot was determined by expert opinion and generalized to the entire work unit. Climatic parameters of rainfall, evaporation, and temperature were studied using data from five meteorological stations over a statistical period of 30 years (1990–2020). The salinity level, water table depth, sodium absorption ratio (SAR), and total dissolved solids (TDS) of the ground water were studied using data from 42 wells over the same statistical period.

Using topographic and geological maps, field visits, interpretation of aerial images, and multispectral and panchromatic bands of satellite imagery obtained from Landsat Thematic Mapper, we were able to identify glacies and playa geomorphological units and their various facies. This was due to the low slope and limited changes in aspect of the area. Ultimately, we identified 14 work units based on geomorphological facies (Appendix A). Wind and water erosion were evaluated using Iran Research Institute of Forest and Rangelands (IRIFR) (Boali et al. 2019) and Erosion Potential Method (EPM) (Gavrilovic, 1988) experimental models, respectively. Information related to erosion models was collected in each of the work units during the field visits and then analysed. The study area is divided into 14 work units, which were classified according to erosion potential using Tables 1 and 2.

## 2.3. Study area Google Earth Engine (GEE)

The computing platform called Google Earth Engine (GEE) was introduced by Google in 2010 (Meng et al., 2021), and has since then been utilized extensively by researchers for obtaining data in various fields including climate, change detection, wetland

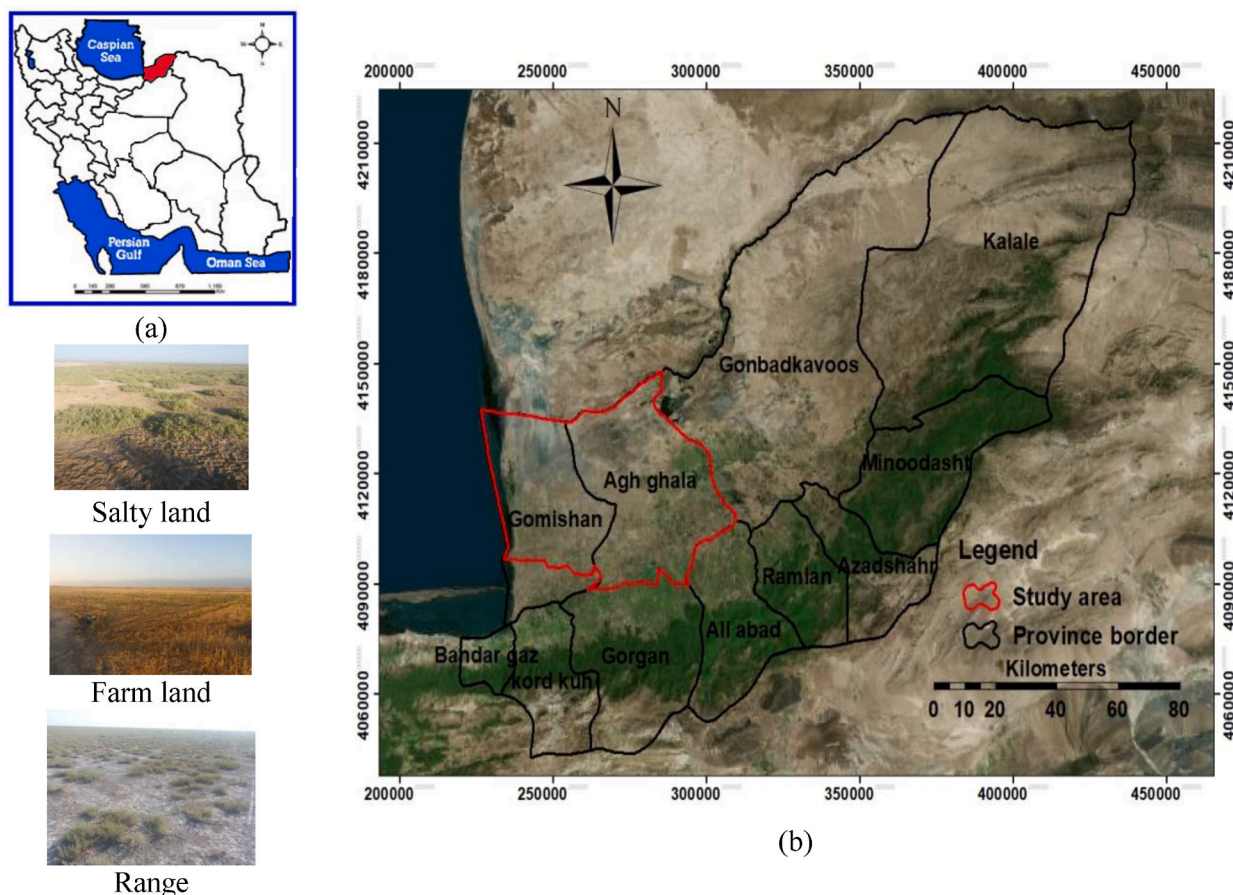


Fig. 1. The location of the studied area on the map of Iran (a) and Satellite image of Golestan province (b).

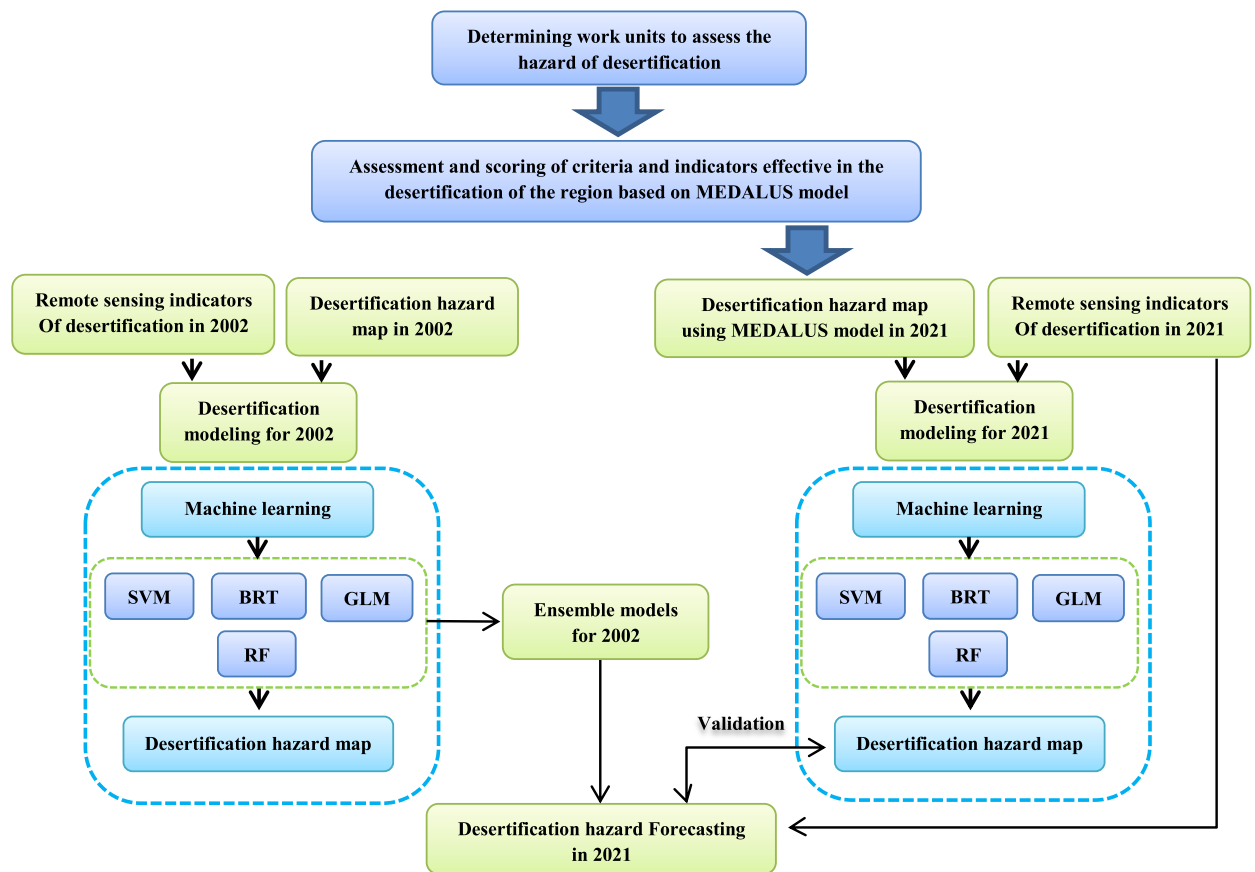


Fig. 2. Methodological flowchart for this study.

mapping, and land-use and land-cover change detection, particularly in remote sensing (Meng et al., 2021). This platform has proven to be a cost-effective and time-efficient tool for acquiring comprehensive information, which was previously unattainable at such a large scale (Midekisa et al., 2017; Huang et al., 2017). The GEE system is equipped with capabilities for fast and extensive monitoring of desertification in the long term. For this study, the atmospheric and geometric corrections were applied to Landsat Tier 1 surface reflectance images, and cross-calibration among different sensors was conducted (Wulder et al., 2008; Dwyer et al., 2018). Landsat images from 2002 to 2021 were utilized to extract remote sensing indicators and to model desertification.

#### 2.4. Desertification assessment using MEDALUS model

To evaluate the desertification situation in the region using the MEDALUS method, six criteria that have an impact on the desertification process were identified based on the SMART approach (E-SMART key Indicators should be E:Economic, S: Specific, M: Measurable, A: Achievable, R: Relevant, and T: Time-bound). These criteria include soil quality, climate quality, groundwater quality, vegetation quality, erosion quality, and management and policy quality (Table 3).

Each criterion was further evaluated using a set of indicators, and a score between 100 and 200 was assigned to each indicator based on its situation in each work unit (Girdano et al., 2002; Appendix B). The geometric mean of the indicators was then used to determine the score for each criterion using Eq. (1). The geometric mean of the criteria scores was used to determine the intensity of desertification in each work unit. Finally, the scores were classified into four classes, low (100–120), moderate (121–135), severe (136–153), and very severe (>153), to create a desertification hazard map.

Table 1

Classification of sedimentation and wind erosion potential in the model proposed by the IRIFR(Boali et al. 2019).

Erosion class	Qualitative erosion status	Score ranges	Sedimentation (ton/km <sup>2</sup> /year)
I	Very low	0–25	250>
II	Low	25–50	250–500
III	Moderate	50–75	500–1500
IV	High	75–100	1500–6000
V	Very high	100>	6000<



**Table 2**

Classification of sedimentation and water erosion potential in the model proposed by the EPM (Gavrilovic, 1988).

Erosion class	Qualitative erosion status	Limit values Z	Sedimentation (m <sup>3</sup> /km <sup>2</sup> /year)
I	Very low	0.19 > Z	64–170
II	Low	0.4 > Z > 0.2	171–437
III	Moderate	0.7 > Z > 0.41	438–1030
IV	High	1 > Z > 0.71	1031–1764
V	Very high	Z > 1	1765<

**Table 3**

The criteria and indicators of desertification assessment in MEDALUS model.

Number	Criteria	Indicators
1	Soil quality	Soil Texture, Electrical Conductivity (EC), Drainage
2	Climate quality	Rainfall (mm), Drought Index, Continuation of drought
3	Groundwater quality	Electrical Conductivity (EC), Sodium Absorption Ratio (SAR), Total Dissolved Solids (TDS), Depth of Groundwater
4	Vegetation quality	Vegetation percentage, Protection against erosion, Resistance against drought
5	Erosion quality	Wind erosion class in IRIFR method, Water erosion class in EPM method
6	Management and Policy quality	Agricultural lands      The quality of agricultural operations Irrigation quality Mines      Exploitation of mines Range lands      Degradation rate of Range lands Grazing pressure Implementation of protection policies

$$W_X = (W_1 * W_2 * \dots * W_n)^{1/n} \quad (1)$$

$W_X$ : Score for each criterion

$W$  (1, 2, ...n): Score for each indicator

$n$ : Number of indicators

## 2.5. Remote sensing indicators for desertification modeling

After using the MEDALUS model to estimate desertification, the study area's most influential indicators will be determined. Initially, a literature review will be conducted to identify effective indicators for desertification in the region, and remote sensing indicators will be considered for each. The remote sensing indicator with the highest correlation to field data will then be utilized for desertification modeling. To select the best indicators, criteria such as Pearson's Correlation Coefficient, Root Mean Squared Error (RMSE), Index of agreement (d) and Coefficient of Determination ( $R^2$ ) will be employed.

## 2.6. Desertification modeling using machine learning algorithms

To minimize spatial correlation, we selected pixel-based samples using a combination of intensive field visits, prior knowledge from MEDALUS desertification maps, and visual interpretation of high-resolution satellite images available on Google Earth. We randomly selected 100 samples from the study area, with 50 samples in areas where desertification had occurred and another 50 samples in areas where it had not yet occurred. We randomly split the samples into a training group (70%) and a testing group (30%). We used four machine learning algorithms – Support Vector Machine (Joshi et al., 2019; Arabameri et al., 2020), Random Forest (RF) (Breiman, 2001), Gradient Boosting Machine (GBM) (Cha et al., 2021; Park et al., 2016), and generalized linear models (GLM) (Mohammed et al., 2020; Chan and Pan 2021) implemented in the sdm R package (Naimi and Araújo, 2016), and each method was repeated three times to ensure consistent classifier performance. To evaluate the models' accuracy, we used the Kappa coefficient, Receiver Operating Characteristic (ROC), and True Skill Statistic (TSS) derived from the confusion matrix, with the diagonal representing the number of correctly classified pixels (Foody and Giles, 2002). The Kappa coefficient assesses overall accuracy, with higher values indicating better agreement between the model and ground truth data (Congalton and Mead, 1983). The ROC curve represents the model's accuracy, with an ideal model having a large area under the curve (AUC) ranging from 0.5 to 1 (Park et al., 2016; Rahmati et al., 2016). We categorized the AUC into excellent (0.9–1), very good (0.8–0.9), good (0.7–0.8), middle (0.6–0.7), and poor (0.5–0.6) classes for qualitative and quantitative correlation (Yesilnacar and Topal, 2005; Devkota et al., 2013). TSS is defined as  $TSS = \text{sensitivity} + \text{specificity} - 1$ , with sensitivity related to correctly predicted values and specificity related to values not correctly predicted (Allouche et al., 2006). The TSS classes are poor (less than 0.2), moderate (0.2–0.6), and good (greater than 0.6). We removed the poor-performing models and used the remaining models to predict desertification.

## 2.7. Ensemble forecasting of desertification

The process of ensemble modeling involves combining the results of individual models to improve predictive accuracy and deal with model-based uncertainty (Araújo and Mark, 2007), which is becoming increasingly popular among Modelers who work with data mining models (Ebrahimi et al. 2023). This approach involves estimating the weights of each model based on their learning skills and

**Table 4**

The scores of various desertification indicators used in MEDALUS model over 14 work units.

Geomorphological units	Work units	The Score of desertification criteria						Geometric mean of the scores	Desertification status
		Management and policy quality	Erosion quality	Vegetation quality	Soil quality	Groundwater quality	Climate quality		
Playa	Wetlands (swampy lands)	153	150	146	167	121	120	141	Severe
	Coastal sediments	140	132	151	140	121	120	133	Moderate
	Saline and wetland lands	145	174	152	154	121	120	143	Severe
	Saline and wetland lands around the playa	146	174	134	160	131	120	143	Severe
Glaciers	Atrak alluvial sediments	152	179	152	155	118	128	146	Very severe
	Saline lands with Sabkha morphology	169	174	147	169	118	128	155	Very severe
	Saline and wetland lands	173	162	151	170	118	128	155	Very severe
	Longitudinal sand dune	139	167	151	144	118	128	140	Severe
	Barkhani dune	139	167	151	137	118	128	139	Severe
	Barren lands	190	165	168	140	118	128	154	Very severe
	Mahuri hill lands	145	117	145	129	118	128	130	Moderate
	Flood plain	170	129	141	140	129	126	134	Severe
	Mahuri hill lands	130	114	143	123	120	126	125	Moderate
	Old alluvial sediments	128	114	143	118	118	126	124	Moderate
Average		151	151	148	146	120	125	140	Severe

Note. Scores close to 200 in the MEDALUS model indicate severe.

adaptability, and then calculating the weighted average of the ensemble model to produce the final result (Chen et al., 2020). Ensemble modeling is an effective way to reduce uncertainty in forecasting by using combined forecasts instead of relying on a single modeling method (Naimi et al., 2022). In this study, four machine learning models were used to predict desertification using remote sensing indices and information about desert areas in 2002 and 2021. An ensemble model was then developed using the weighted average of the individual models in the sdm statistical package (Naimi and Araújo, 2016). The ensemble model developed using data collected in 2002 was used with remote sensing data from 2021 to predict desertification, and the resulting map was validated against the actual desertification map of 2021.

### 3. Results

#### 3.1. Assessment of desertification using MEDALUS model

The MEDALUS model was used to identify the most important factors contributing to desertification in the study area. Based on the model results, the management and policy criteria (score 151), erosion criteria (score 151), vegetation (score 148), and soil (score 146) were found to be the most significant factors (Table 4 and Fig. 3). The region's heavy soil texture (clay loam), limited vegetation due to natural and abnormal causes, and lack of organic matter have led to a significant increase in erosion. The mutual effects of the three criteria of erosion, vegetation, and soil, along with weak management practices, are the main factors contributing to the current conditions and spread of desertification in the region (see Fig. 4).

In addition, the most important indicators of desertification include plants' resistance to drought (score 162), conservation operations (score 158), and soil salinity (score 155). These indicators have accelerated the desertification process in abandoned lands, saline and wetland regions, and saline lands in the northeastern parts of the study area. Based on the MEDALUS model, 27% of the region falls under the Low desertification class (southern part), 37% in the Moderate class (central part), 24% in the Severe class (northern and eastern parts), and 12% in the Very Severe desertification class (northeastern part of the region) (Fig. 3).

#### 3.2. Selection of remote sensing indicators for desertification modeling

To model desertification using remote sensing, a comprehensive analysis of various sources was conducted to select eight

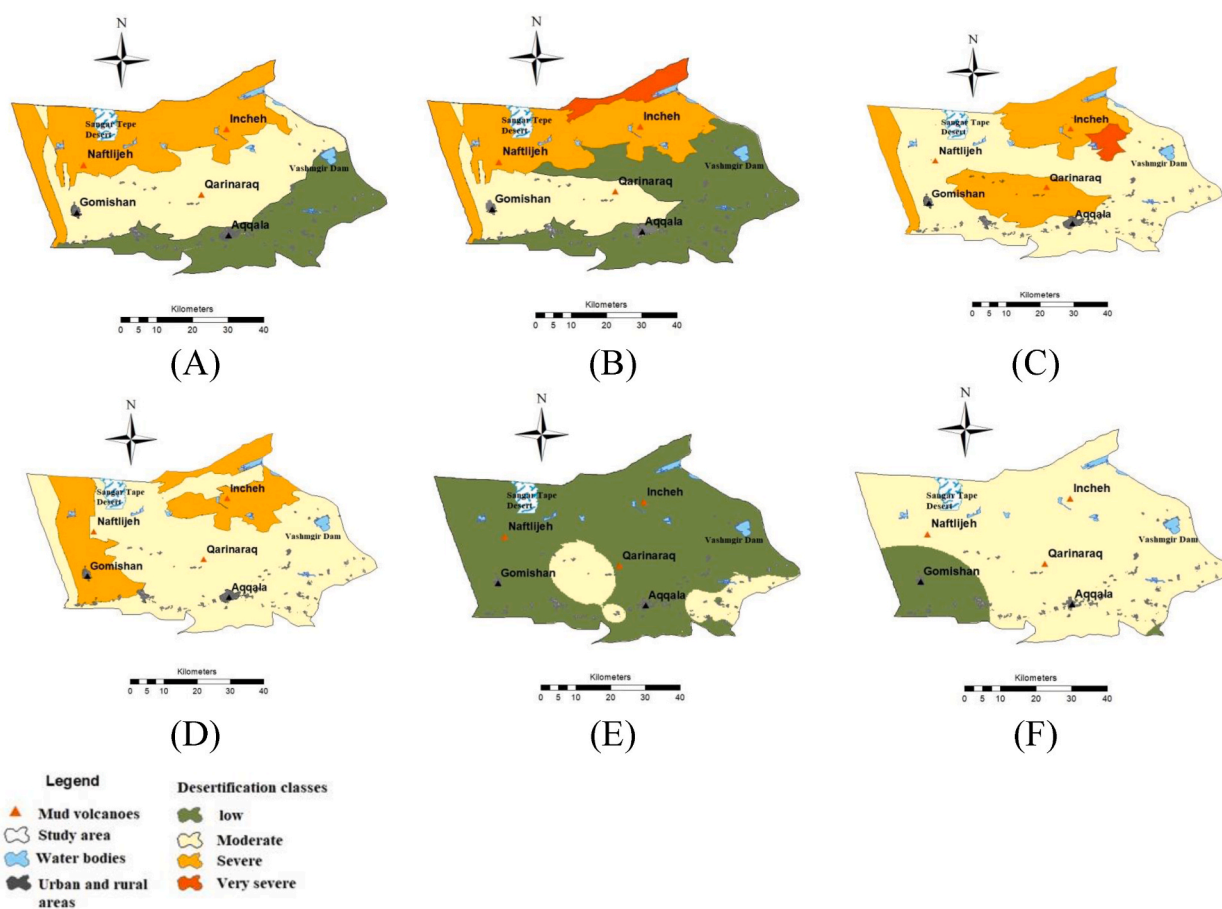


Fig. 3. Map of desertification criteria in the MEDALUS model: A-Soil; B-Erosion; C-Management and policy; D-Vegetation; E-Groundwater; and F-Climate.

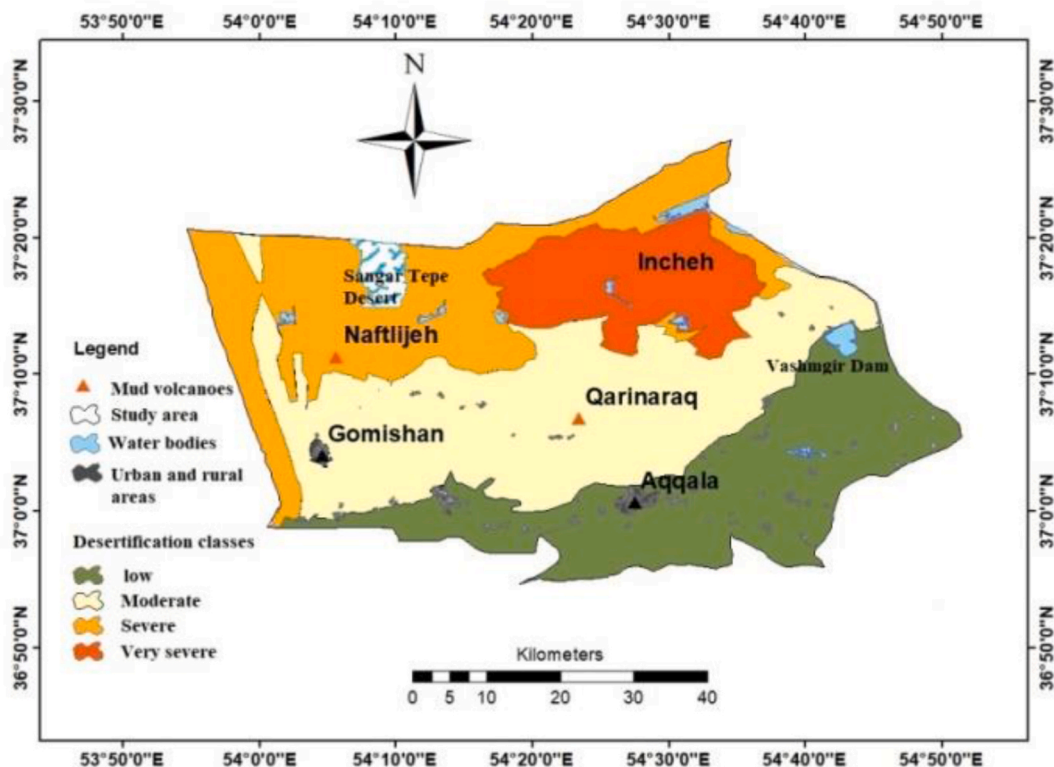


Fig. .4. Desertification status in Northwest of Golestan province, Iran based on the MEDALUS model.

indicators, including soil texture and salinity, precipitation amount, vegetation cover percentage, wind and water erosion, and land use change (Table 5), in addition to the criteria identified by the MEDALUS model. To select each of these indices, several remote sensing indices were examined and the index that had the highest correlation with the field data was selected for modeling.

### 3.3. Desertification modeling

After preparing maps of remote sensing indicators (see Fig. 8 in Appendix C), the desertification modeling was performed for the years 2002 and 2021, and the results of the four models used to evaluate desertification in 2002 were somewhat similar. The RF and SVM models predicted the northeastern regions, while the GLM and GBM models predicted the northern and northeastern regions of the study area under the hazard of desertification (Fig. 5). To evaluate the modeling results, statistical parameters such as kappa coefficient, receiver operating characteristic (ROC) curve, and true skill statistics (TSS) were used (Table 6). Based on the modeling conducted in 2002, the RF and SVM models performed better than the GLM and GBM models. However, in general, the SVM model

**Table 5**  
Selection of indicators based on the degree of correlation with ground surface data.

Medalus model indicators	Remote sensing indicators	Ground surface data	Correlation rate between satellite indicators and ground surface data				Reference
			R <sup>2</sup>	d	RMSE	Pearson coefficient	
Soil texture	TGSI	Soil surface profile	0.56	0.62	0.78	0.85	Xiao et al. (2006); Meng et al. (2021)
EC	NDSI		0.63	0.88	8.54	0.88	Engdawork et al. (2016), Dehni and Lounis (2012)
Rainfall	Chrips	synoptic stations	0.51	0.78	214.53	0.67	Park et al. (2016)
Vegetation percent	NDVI	Vegetation percentage in plots	0.71	0.71	1.39	0.78	Jiang et al. (2019); Lamchin et al. (2016)
Wind erosion	WEHI model = /NDMI (wind speed* MBI)	IRIFR model map based on area data	0.56	0.85	0.69	0.77	Yang and Leys (2014)
Water erosion	ICONA model = (Geology * Slope) * (Land use * NDVI)	EPM model map based on area data	0.57	0.69	0.55	0.59	Bayramin et al. (2003)
Management	Land use changes	Map of ground evidence	0.66	0.82	0.61	0.82	Wijitkosum (2015)



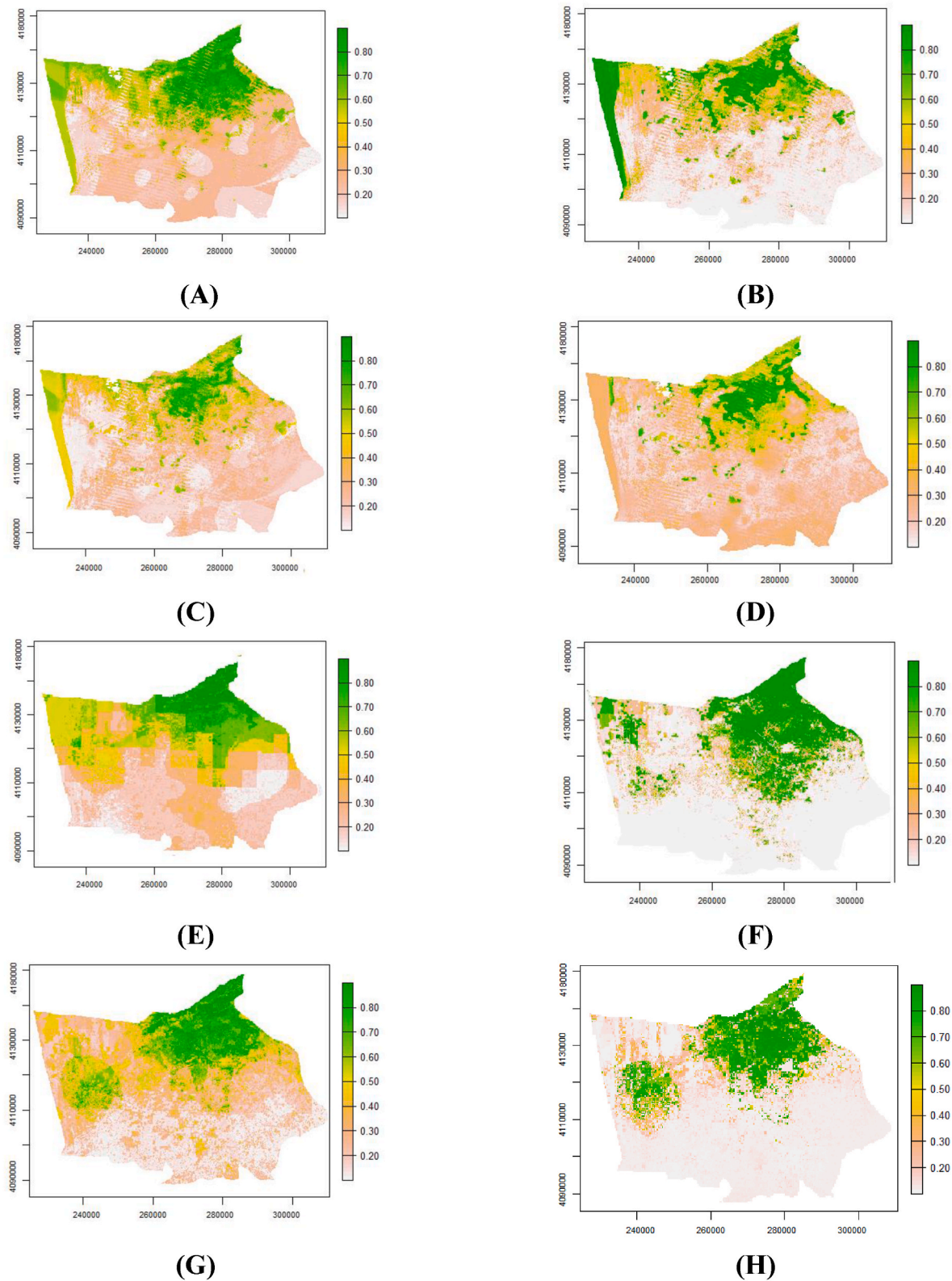


**Fig. 5.** Maps of desertification in 2002 and 2021 in Northeastern Iran using different models in the SDM package. A, B, C and D are models GBM, GLM, RF and SVM in 2002 respectively and E, F, G, and H are models GBM, GLM, RF and SVM in 2021, respectively.

with  $AUC = 0.91$ ,  $TSS = 0.93$ , and  $Kappa = 0.86$  was found to be the best model, and the GLM model with  $AUC = 0.79$ ,  $TSS = 0.58$ , and  $Kappa = 0.61$  was the weakest model. The results obtained from the four models in 2021 were different. The GBM model predicted the northern areas of the region as areas with severe desertification, while the GLM model predicted the northeastern areas and somewhat scatteredly the northwestern areas as areas with severe desertification. The RF and SVM models identified the northeastern and western regions of the study area as desert areas, but the RF model predicted the intensity of desertification in the region more accurately than the SVM model. The results of the performance evaluation parameters of the models in 2021 showed that the RF model was the best model with  $AUC = 0.94$ ,  $TSS = 0.94$ , and  $Kappa = 0.90$ , while the GLM model also presented the weakest performance with  $AUC = 0.77$ ,  $TSS = 0.77$ , and  $Kappa = 0.65$  (Table 6).

### 3.4. Forecast and validation of desertification

To forecast desertification in 2021, we used an ensemble of desertification models that combined the results from 2002 with remote sensing indicators from 2021. Our prediction showed that the northeastern regions and some central areas of the study area were affected by desertification, as well as the western areas near the Gomishan wetland (Fig. 6A). We then validated the ensemble model by comparing its predictions with the actual 2021 desertification map (Fig. 6B). Our validation results showed that the ensemble model had high accuracy, with an  $AUC$  of 0.86,  $TSS$  of 0.84, and  $Kappa$  of 0.78, indicating that the model performed well in predicting desertification (see Fig. 7).

### 3.5. Relative importance of variables

In the four models used to evaluate desertification in 2002, the NDSI index (soil salinity) was found to be the most important indicator in the desertification of the region. Ahmadi (1381) identified land salinization and land swamping as the two most important factors in the desertification of Agh Qola and Gamishan plains. The swamping process plays a fundamental role due to its increasing impact on other variables, particularly soil salinity in the region.

In 2021, the land use change index was identified as the most important indicator in the desertification of the region. The increase in population and subsequent demand for agricultural products are among the main causes of land use change in recent years. The south of the examination area is one of the main centers of dry wheat cultivation in Iran, and the cultivated area has increased by a factor of 10 over the last 20 years in this area. This change in land use is an important factor contributing to the desertification of the region.

## 4. Discussion

### 4.1. Assessment of desertification using MEDALUS model

The assessment of desertification using the MEDALUS model proved to be an effective approach for understanding the extent and severity of desertification in Northeast Iran. The results revealed that a significant portion of the region, specifically the North and Northeast, falls within the severe and very severe desertification class, accounting for 36% of the region. The major cause of this regression is poor management practices, resulting in the loss of vegetation cover and the exposure of surface soil, leading to increased soil erosion. These findings are consistent with previous studies, such as Akbari et al. (2016), which identified soil, vegetation, and management and policy as the most important criteria for desertification in the west of Golestan province.

Inappropriate management measures in the region, such as unprincipled road construction, have also contributed to critical conditions by causing the accumulation of surface water waste and salt after evaporation. Changes in the physical and chemical properties of soil, such as increasing soil salinity, reducing soil organic matter, and destroying soil structure, have been identified as accelerators of the desertification process (Castellano and Valone, 2007). Another contributing factor is the rise of the underground water level, caused by fluctuations in the water level of the Caspian Sea, leading to increased soil salinity and swamping of the land, thereby accelerating the process of desertification in the soil (Jafari and Bakshandehmehr, 2016).

Based on the results, the resistance index of plants against drought was recognized as the most important index in the diagnosis and investigation of desertification in the region. In other words, this index is considered to measure and analyze the resistance of plants in the region against drought, and it can be cited to what extent the climate of the region can affect desertification. Researchers have shown in their studies that climate change can have a great impact on increasing desertification. Therefore, examining drought indicators can help us in better management of the region and provide suitable solutions to deal with desertification (Santos et al., 2022; Bohn et al., 2021).

**Table 6**

Performance evaluation of models based on various indicators in the period of 2002 and 2021.

Methods		AUC	TSS	KAPPA
GLM	2002	0.79	0.58	0.61
	2021	0.77	0.77	0.65
RF	2002	0.88	0.92	0.82
	2021	0.94	0.94	0.90
GBM	2002	0.82	0.88	0.67
	2021	0.85	0.88	0.72
SVM	2002	0.91	0.93	0.86
	2021	0.92	0.96	0.88

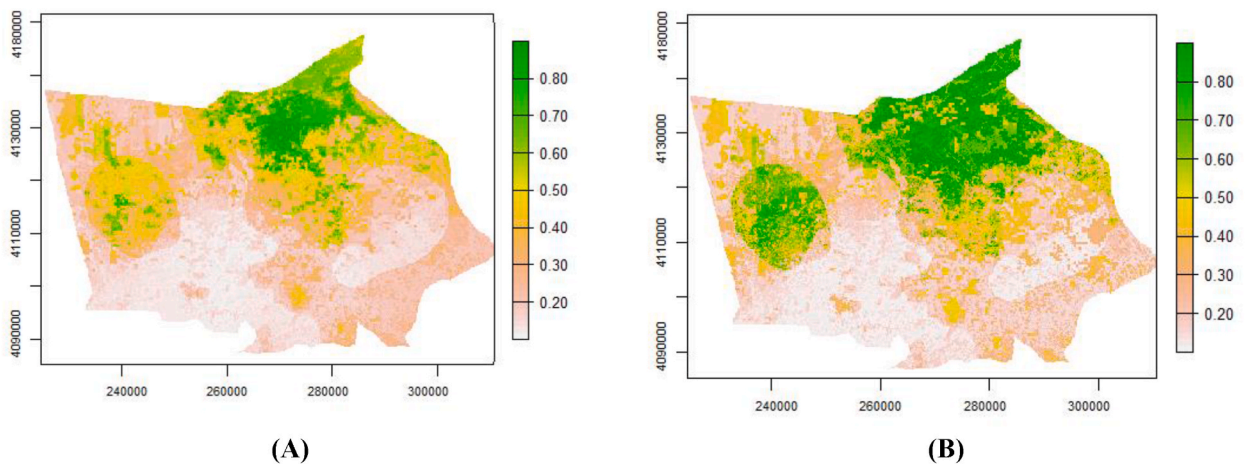


Fig. 6. A – Desertification Forecast map in 2021. B – Map of desertification in 2021 using the ensemble model.

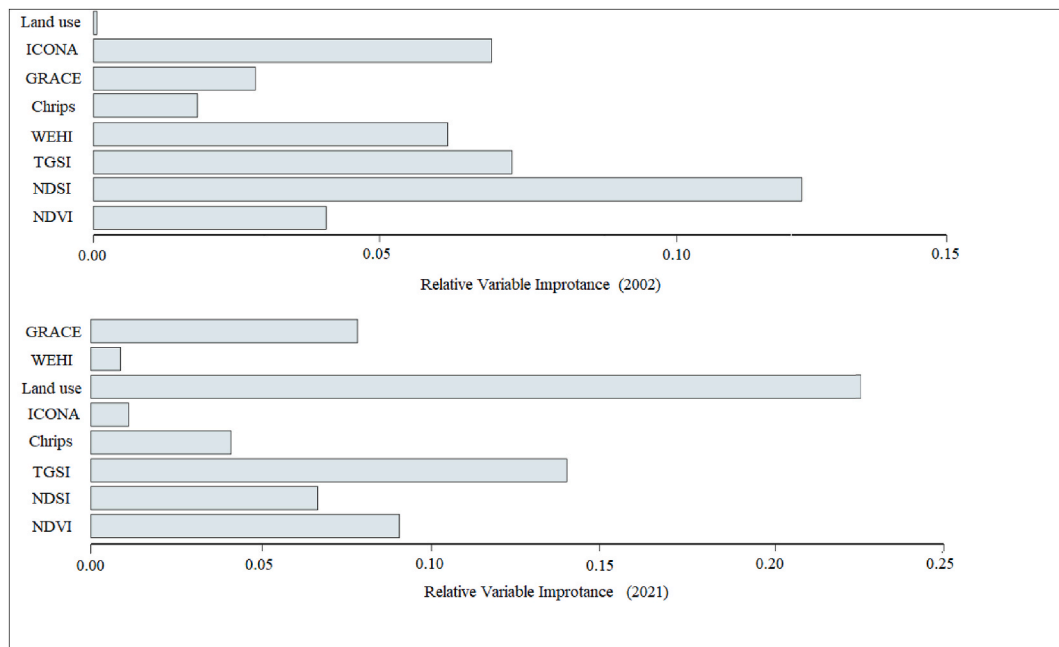


Fig. 7. Importance of variables in the study area in 2002 and 2021.

#### 4.2. Selection of remote sensing indicators

To evaluate soil texture, TGSI index was chosen based on the literature review, as the coarsening of surface soil grains is a visible sign of land degradation and can be used as an indicator to monitor desertification (Xiao et al., 2006; Meng et al., 2021). Among the remote sensing indices explored to assess soil salinity (NDSI, VSSI and SI), the Normalized Difference Salinity Index (NDSI) was selected due to its high Pearson correlation coefficient (0.88), low root mean square error (RMSE = 8.54), Index of agreement high ( $d = 0.88$ ) and appropriate coefficient of determination ( $R^2 = 0.59$ ) (Dehni and Lounis, 2012; Asfaw et al., 2018). After analyzing satellite data from GPM, PERSIANN, TRMM, and Chrips, the Chrips satellite data was found to be suitable for assessing the amount of precipitation in the region based on correlation criteria (Table 5).

To evaluate vegetation cover, four indicators were considered including Soil Adjusted Vegetation Index (SAVI), Difference Vegetation Index (DVI), Enhanced Vegetation Index (EVI), and NDVI, and the NDVI index had the highest correlation with ground data and was therefore chosen for modeling. Young and Leys (Yang and Leys, 2014) first used the Wind Erosion Hazard Index (WEHI) model to assess wind erosion in Australia. This model includes three indicators of wind speed, soil moisture and bare soil. Wind speed information is obtained based on anemometer station and soil moisture and bare soil based on remote sensing data. The high correlation coefficients between the WEHI model, which is based on remote sensing, and the IRIFR model, which is based on field data, indicate

the high capability of this model in estimating wind erosion. The Institute Conservation Of Nature (ICONA) remote sensing model was used to evaluate water erosion. This model, presented by the Spanish Institute Conservation Of Nature, has four geological indicators, slope, land use and percentage of vegetation. Based on the obtained results, this model has a high correlation with the EPM experimental model (Table 5). The map of land use changes was also used as a remote sensing index to investigate the management and policy factor in desertification evaluation. To validate this map, it was correlated with the ground evidence map generated during field visits and using Google Earth images. As for groundwater studies, interpolation of well data was used as the application of remote sensing in groundwater studies is limited.

#### 4.3. Modeling and prediction of desertification

To model and predict desertification, eight remote sensing indicators were selected based on the MEDALUS model and a review of sources. Due to the limitation of remote sensing application in groundwater studies, Interpolation of well data was used, while recently the use of GRACE satellite data has been developed for groundwater assessment. GRACE satellite data is used to investigate changes in groundwater depth. But the data of this satellite has been updated until 2017(Moiwo et al., 2012). These indicators provide an overall assessment of desertification and examine it from different aspects. Four methods from the sdm R package were used to model desertification in 2002 and 2021. The SVM model was found to perform best in 2002, while the RF model performed best in 2021. The SVM model was effective because it created the greatest amount of separation between the data (Vapnik, 1995), which allowed it to divide the data into distinct groups. The RF model was successful because it avoided overfitting by using random subsets of features to create smaller trees. However, compared to other machine learning algorithms, the RF model is more complex and time-consuming (Pourghasemi et al., 2013; Ge et al., 2020; Meenal et al., 2021). Uncertainty in the models confirms the necessity of using a hybrid approach, reducing uncertainty in predictions (Naimi and Araújo, 2016). To predict desertification in 2021, a combined model was used, which utilized the desertification model of 2002 and remote sensing indicators of 2021. Although the model correctly predicted the areas affected by desertification, it underestimated the intensity of desertification in those areas. The combined model was particularly effective in predicting the northeastern regions of the area, where abandoned lands, saline and swamp lands, and saline lands have accelerated the process of desertification.

## 5. Conclusion

Desertification has become a significant challenge in many countries, affecting critical environmental components such as soil, water, and vegetation cover. This study has evaluated, modeled, and forecasted desertification in a region using four statistical models. The accuracy of the models was evaluated using three statistics, Kappa, AUC, and TSS, which identified the best model. The results of the ensemble model showed a trend of desertification from west to east in the region. To reduce the uncertainty in forecasts, the use of a superior model and an ensemble approach is a suitable solution. By emphasizing the results of the ensemble model, along with planning, management, and applying corrective methods in the identified areas, we can reduce desertification and improve the condition of the region. The study identified soil salinity variables and land use change as the most influential factors in increasing desertification in the region. By focusing on these variables, the cost and time used for research can be reduced, and the prediction accuracy of the models can be increased. Therefore, this study highlights the need to model and predict desertification for better management of natural and man-made ecosystems and long-term planning.

#### Funding sources

This research did not receive any specific grant from funding agencies in the public, commercial, or not-for-profit sectors.

#### CRediT authorship contribution statement

**Abdolhossein Boali:** Conceptualization, Data curation, Formal analysis, Investigation. **Hamid Reza Asgari:** Supervision. **Ali Mohammadian Behbahani:** Investigation. **Abdolrassoul Salmanmahiny:** Methodology. **Babak Naimi:** Software, Validation.

#### Declaration of competing interest

The authors declare that they have no known competing financial interests or personal relationships that could have appeared to influence the work reported in this paper.

#### Data availability

Data will be made available on request.



## Appendix A

**Table 7**

Distribution of frequency percentage of work units in the study area

Unit	Unit code	Facies	Area (hectares)	Frequency	Code facies
Playa	1	Wetlands (swampy lands)	14484.42	4.96	1-1-1
		Coastal sediments	25718.72	8.81	1-1-2
		Saline and wetland lands	9124.87	3.12	1-2-1
		Saline and wetland lands around the playa	27874.87	9.55	1-3-1
Pediment	2	Atrak alluvial sediments	11981.39	4.1	2-1-1
		Saline lands with Sabkha morphology	11,497	3.94	2-1-2
		Saline and wetland lands	18765.78	6.43	2-1-3
		Longitudinal sand dune	3307.94	1.13	2-1-4
		Barkhani dune	644.55	0.22	2-1-5
		Barren lands	5419.90	1.85	2-1-6
		Mahuri hill lands	43272.1	14.83	2-1-7
		Flood plain	40569.43	13.91	2-2-1
		Mahuri hill lands	49586.11	17	2-2-2
		Old alluvial sediments of Gorgan River	29373.11	10.15	2-2-3

## Appendix B

**Table 8**

Classes and assigned weights for the 20 desertification indices in Northeast Iran

Soil quality ( $W_S$ ) = (Soil Texture $\times$ EC $\times$ ) <sup>1/3</sup>						
	EC (ds/cm)	Assigned weight	Texture	Drainage	Assigned weight	
1	0–8	100–120	L · SCL · SL LS · CL	Good	100–125	
2	8–16	120–140	SC· SiL ·SiCL	Moderate	125–150	
3	16–32	140–160	Si · c · sic	Weak	150–175	
4	32–100	160–180	S	Very weak	175–1200	
5	>100	180–200				
Groundwater quality (WG) = (EC $\times$ SAR $\times$ TDS $\times$ Decline in Groundwater) <sup>1/4</sup>						
	EC (μ mho/cm)	Decline in groundwater (cm)	Assigned weight	SAR (meq L <sup>−1</sup> )	TDS (Mg/l)	Assigned weight
1	250>	0–10	100–120	10>	500 >	100–125
2	250–750	10–20	120–140	10–18	1000–500	125–150
3	750–2250	20–30	140–160	18–26	2000–1000	150–175
4	2250–5000	30–50	160–180	26<	2000 <	175–200
5	5000<	50 <	180–200			
Climate quality ( $W_C$ ) = (Drought Index $\times$ Rainfall $\times$ Aridity Index) <sup>1/3</sup>						
	Drought Index	Rainfall	Continuation of drought			Assigned weight
1	>0.65	300<	1–3 years			100–125
2	0.45–0.65	150–300	4–5 years			125–150
3	0.2–0.45	150–75	6–7 years			150–175
	<0.2	<75	More than 7 years			175–1200
Vegetation quality ( $W_V$ ) = (Vegetation Cover $\times$ Drought Resistance $\times$ Erosion Protection) <sup>1/3</sup>						
	Erosion Protection and Drought Resistance			Vegetation Cover	Assigned weight	
1	Gardens, shrubs and evergreen rangelands			50<	100–125	
2	Rangelands and Shrubbery permanent			35–50	125–150	
3	Annual crops, cereals, grasslands annual			10–35	150–175	
4	Bare and barren land			10>	175–1200	
Soil erosion quality ( $W_{Er}$ ) = (Wind Erosion $\times$ Water Erosion) <sup>1/2</sup>						
	Wind Erosion (IRIFR)		Water Erosion (EPM)		Assigned weight	
1	I و II		I و II		100–125	
2	III		III		125–150	
3	IV		IV		150–175	
4	V		V		175–1200	
Management and policy quality ( $W_M$ ) = (Rangeland land use $\times$ Agricultural land use) <sup>1/2</sup>						

(continued on next page)

Table 8 (continued)

Management and policy quality ( $W_M$ ) = (Rangeland land use $\times$ Agricultural land use) <sup>1/2</sup>				
Agricultural land use = (Quality of agricultural operations $\times$ Irrigation method and water quality $\times$ Extent of protection operations) <sup>1/3</sup>				
Irrigation method and water quality		Assigned weight	Quality of agricultural operations	Assigned weight
Agricultural land use = (Quality of agricultural operations $\times$ Irrigation method and water quality $\times$ Extent of protection operations) <sup>1/3</sup>				
Irrigation method and water quality		Assigned weight	Quality of agricultural operations	Assigned weight
1	Use of modern irrigation methods, proper irrigation water quality	100–125	Cultivation of native varieties, no use of chemical fertilizers, limited mechanization, suitable fallow	100–135
2	Use of modern irrigation methods, inadequate irrigation water quality	125–150	Cultivation of modified varieties, use of chemical fertilizers, mechanization in necessary cases	135–175
3	Use of traditional irrigation methods, relatively good irrigation water quality	150–175	Cultivation of improved varieties, use of fertilizers and pesticides, unlimited and intense mechanization, no fallow land	175–200
4	Use of traditional irrigation methods, relatively good irrigation water quality	175–1200		
Rangeland land use = (grazing pressure $\times$ Degree of pasture destruction $\times$ Extent of protection operations) <sup>1/3</sup>				
Degree of pasture destruction (Potential to actual capacity ratio)			grazing pressure (The ratio of available livestock to the pasture capacity)	Assigned weight
1	1–1.5		0–1	100–125
2	1.5–2		1–1.5	125–150
3	2–5		1.5–2	150–175
4	<5		<2	175–1200
Extent of protection operations (All land uses)				Assigned weight
1	More than 70% of the area under protection operations			100–125
2	30–70% of the area under protection operations			125–150
3	Less than 30% of the area under protection operations			150–175
4	Failure to implement any protection operations			175–1200

## Appendix C

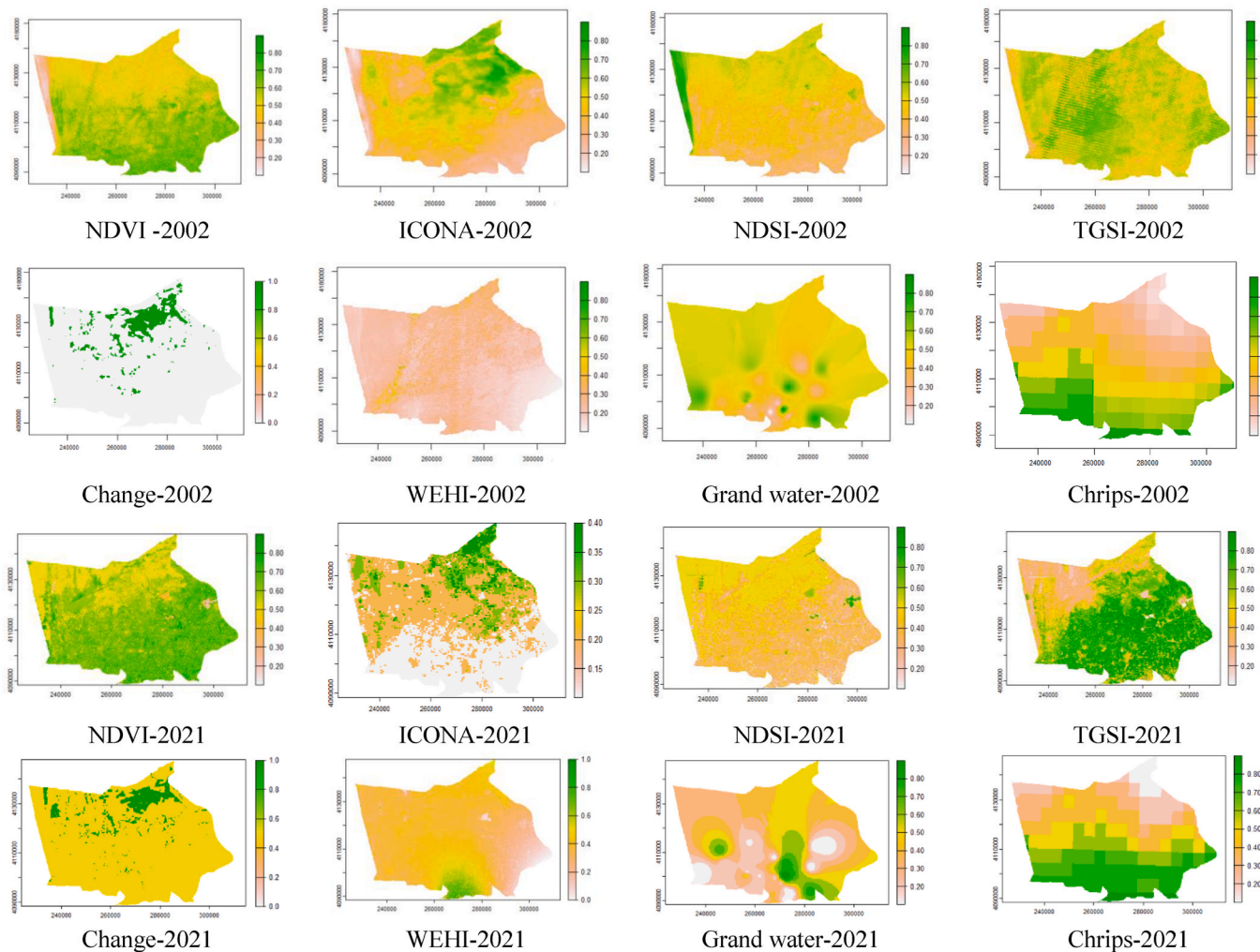


Fig. 8. Remote sensing indicators for desertification modeling in 2002 and 2021

## References

- Abuzaid, Ahmed S., Abdelatif, Abdelatif D., 2022. Assessment of desertification using modified MEDALUS model in the North Nile Delta, Egypt. *Geoderma* 405. <https://doi.org/10.1016/j.geoderma.2021.115400>.
- Afzali, Sayed Fakhreddin, Ali, Khanamani, Maskooni, Ehsan Kamali, Berndtsson, Ronny, 2021. Quantitative assessment of environmental sensitivity to desertification using the modified medalus model in a Semiarid area. *Sustainability* 13 (14). <https://doi.org/10.3390/su13147817>.
- Akbari, M., Ownegh, M., Asgari, H.R., Sadoddin, A., Khosravi, H., 2016. Desertification risk assessment and management program. *Global J. Environ. Sci. Manag.* 2 (4), 365–380. <https://doi.org/10.22034/gjesm.2016.02.04.006>.
- Allouche, Omri, Tsoar, Asaf, Ronen, Kadmon, 2006. Assessing the accuracy of species distribution models: prevalence, kappa and the true skill statistic (TSS). *J. Appl. Ecol.* 43 (6), 1223–1232. <https://doi.org/10.1111/j.1365-2664.2006.01214.x>.
- Arabameri, Alireza, Asadi Nalivan, Omid, Saha, Sunil, Roy, Jagabandhu, Pradhan, Biswajeet, Tiefenbacher, John P., Ngo, Phuong Thao Thi, 2020. Novel ensemble approaches of machine learning techniques in modeling the gully erosion susceptibility. *Rem. Sens.* 12 (11). <https://doi.org/10.3390/rs12111890>.
- Araújo, Miguel B., Mark, New, 2007. Ensemble forecasting of species distributions. *Trends Ecol. Evol.* 22 (1), 42–47. <https://doi.org/10.1016/j.tree.2006.09.010>.
- Asfaw, Engdawork, Suryabagavan, K.V., Mekuria, Argaw, 2018. Soil salinity modeling and mapping using remote sensing and GIS: the case of Wonji sugar cane irrigation Farm, Ethiopia. *J. Saudi Soc. Agric. Sci.* 17 (3), 250–258. <https://doi.org/10.1016/j.jssas.2016.05.003>.
- Bezerra, F.G.S., Aguiar, A.P.D., Alvalá, R.C.S., Giarolla, A., Bezerra, K.R.A., Lima, P.V.P.S., do Nascimento, F.R., Arai, E., 2020. Analysis of areas undergoing desertification, using EVI2 multi-temporal data based on MODIS imagery as indicator. *Ecol. Indic.* 117. <https://doi.org/10.1016/j.ecolind.2020.106579>.
- Boali, Abdolhossein, Bashari, Hossein, Jafari, Reza, 2019. Evaluating the potential of Bayesian networks for desertification assessment in arid areas of Iran. *Land Degrad. Dev.* 30 (4), 371–390. <https://doi.org/10.1002/ldr.3224>.
- Bohn, Leonardo, Lyra, Gustavo Bastos, Francisco Oliveira-Júnior, José, Zeri, Marcelo, Cunha-Zeri, Giseline, 2021. Desertification susceptibility over Rio de Janeiro, Brazil, based on aridity indices and geoprocessing. *Int. J. Climatol.* 41 (S1), E2600–E2614. <https://doi.org/10.1002/joc.6869>.
- Bouhata, Rabah, Bensekhria, Aida, 2021. Adaptation of MEDALUS method for the analysis depicting desertification in oued Labiod valley (eastern Algeria). *Arabian J. Geosci.* 14 (5). <https://doi.org/10.1007/s12517-021-06679-2>.
- Breiman, Leo, 2001. Random forests. *Mach. Learn.* 45 (1), 5–32. <https://doi.org/10.1109/ICCECE51280.2021.9342376>.

- Budak, Mesut, Günel, Hikmet, İsmail, Çelik, Yıldız, Hakan, Acir, Nurullah, Acar, Mert, 2018. Environmental sensitivity to desertification in northern mesopotamia; application of modified MEDALUS by using analytical Hierarchy process. *Arabian J. Geosci.* 11 (17), 232–243. <https://doi.org/10.1007/s12517-018-3813-y>.
- Castellano, M.J., Valone, T.J., 2007. Livestock, soil compaction and water infiltration rate: evaluating a potential desertification recovery mechanism. *J. Arid Environ.* 71 (1), 97–108. <https://doi.org/10.1016/j.jaridenv.2007.03.009>.
- Cha, Gi Wook, Moon, Hyeun Jun, Kim, young Chan, 2021. Comparison of random forest and gradient boosting machine models for predicting demolition waste based on small datasets and categorical variables. *Int. J. Environ. Res. Publ. Health* 18 (16). <https://doi.org/10.3390/ijerph18168530>.
- Chan, Hing Ling, Pan, Mingling, 2021. Fishing trip cost modeling using generalized linear model and machine learning methods – a case study with longline fisheries in the Pacific and an application in regulatory impact analysis. *PLoS One* 16 (9 September). <https://doi.org/10.1371/journal.pone.0257027>.
- Chen, Karen, Tzu Hsin, Qiu, Chunping, Schmitt, Michael, Zhu, Xiao Xiang, Sabel, Clive E., Prishchepov, Alexander V., 2020. Mapping horizontal and vertical urban densification in Denmark with Landsat time-series from 1985 to 2018: a semantic segmentation solution. *Remote Sens. Environ.* 251 <https://doi.org/10.1016/j.rse.2020.112096>.
- Dehni, Abdellatif, Lounis, Mourad, 2012. Remote sensing techniques for salt affected soil mapping: application to the oran region of Algeria. *Procedia Eng.* 33, 188–198. <https://doi.org/10.1016/j.proeng.2012.01.1193>.
- Devkota, Krishna Chandra, Regmi, Amar Deep, Pourghasemi, Hamid Reza, Yoshida, Kohki, Pradhan, Biswajeet, In Chang, Ryu, Raj Dhital, Megh, Althuwaynee, Omar F., 2013. Landslide susceptibility mapping using certainty factor, index of entropy and logistic regression models in GIS and their comparison at Mugling-Narayanghat road section in Nepal Himalaya. *Nat. Hazards* 65 (1), 135–165. <https://doi.org/10.1007/s11069-012-0347-6>.
- Duan, Hanchen, Wang, Tao, Xue, Xian, Yan, Changzhen, 2019. Dynamic monitoring of aeolian desertification based on multiple indicators in Horqin Sandy land, China. *Sci. Total Environ.* 650, 2374–2388. <https://doi.org/10.1016/j.scitotenv.2018.09.374>.
- Dwyer, John L., Roy, David P., Sauer, Brian, Jenkinson, Calli B., Zhang, Hankui K., Lymburner, Leo, 2018. Analysis ready data: enabling analysis of the Landsat archive. *Rem. Sens.* 10 (9) <https://doi.org/10.3390/rs10091363>.
- Ebrahimi, Elham, Araújo, Miguel B., Naimi, Babak, 2023. Flood susceptibility mapping to improve models of species distributions. *Ecol. Indic.* 157, 111250 <https://doi.org/10.1016/j.ecolind.2023.111250>.
- Elnashar, Abdelrazek, Zeng, Hongwei, Wu, Bingfang, Gebremicael, Tesfay Gebretsadkan, Marie, Khadiga, 2022. Assessment of environmentally sensitive areas to desertification in the blue Nile basin driven by the MEDALUS-GEE framework. *Sci. Total Environ.* 815 <https://doi.org/10.1016/j.scitotenv.2022.152925>.
- Ferrara, Agostino, Kosmas, Constantinos, Salvati, Luca, Padula, Antonietta, Mancino, Giuseppe, Angelo, Nolè, 2020. Updating the MEDALUS-ESA framework for worldwide land degradation and desertification assessment. *Land Degrad. Dev.* 31 (12), 1593–1607. <https://doi.org/10.1002/ldr.3559>.
- Filei, A.A., Slesarenko, L.A., Boroditskaya, A.V., Mishigdorj, O., 2018. Analysis of desertification in Mongolia. *Russ. Meteorol. Hydrol.* 43 (9), 599–606. <https://doi.org/10.3103/S1068373918090066>.
- Foody, Giles, M., 2002. Status of land cover classification accuracy assessment. *Remote Sens. Environ.* [https://doi.org/10.1016/S0034-4257\(01\)00295-4](https://doi.org/10.1016/S0034-4257(01)00295-4).
- Gavrilovic, Z., 1988. *The Use of an Empirical Method (Erosion Potential Method) for Calculating Sediment Production and Transportation in Unstudied or Torrential Streams* (ISBN 0-471-91955-1).
- Ge, Genbatu, Shi, Zhongjie, Zhu, Yuanjun, Yang, Xiaohui, Hao, Yuguang, 2020. Land use/cover classification in an arid desert-Oasis Mosaic landscape of China using remote sensed imagery: performance assessment of four machine learning algorithms. *Global Ecol. Conserv.* 22 <https://doi.org/10.1016/j.gecco.2020.e00971>.
- Guo, Bing, Zhang, Wenqian, Han, Baomin, Yang, Fei, Luo, Wei, He, Tianli, Fan, Yewen, Yang, Xiao, Chen, Shuting, 2020. Dynamic monitoring of desertification in naiman banner based on feature space models with typical surface parameters derived from LANDSAT images. *Land Degrad. Dev.* 31 (12), 1573–1592. <https://doi.org/10.1002/ldr.3533>.
- Huang, Huabing, Chen, Yanlei, Clinton, Nicholas, Wang, Jie, Wang, Xiaoyi, Liu, Caixia, Gong, Peng, et al., 2017. Mapping major land cover dynamics in Beijing using all Landsat images in Google Earth engine. *Remote Sens. Environ.* 202, 166–176. <https://doi.org/10.1016/j.rse.2017.02.021>.
- Jafari, Reza, Bakhshandehmehr, Leila, 2016. Quantitative mapping and assessment of environmentally sensitive areas to desertification in Central Iran. *Land Degrad. Dev.* 27 (2), 108–119. <https://doi.org/10.1002/ldr.2227>.
- Jiang, Liangliang, Jiapaer, Gul, Bao, Anming, Kurban, Alishir, Guo, Hao, Zheng, Guoxiong, De Maeyer, Philippe, 2019. Monitoring the long-term desertification process and assessing the relative roles of its drivers in central Asia. *Ecol. Indic.* 104, 195–208. <https://doi.org/10.1016/j.ecolind.2019.04.067>.
- Joshi, Pratik P., Wynne, Randolph H., Thomas, Valerie A., 2019. Cloud detection algorithm using SVM with SWIR2 and tasseled cap applied to Landsat 8. *Int. J. Appl. Earth Obs. Geoinf.* 82 <https://doi.org/10.1016/j.jag.2019.101898>.
- Lamchin, Munkhnasan, Lee, Jong Yeol, Lee, Woo Kyun, Lee, Eun Jung, Kim, Moonil, Lim, Chul Hee, Choi, Hyun Ah, Kim, So Ra, 2016. Assessment of land cover change and desertification using remote sensing technology in a local region of Mongolia. *Adv. Space Res.* 57 (1), 64–77. <https://doi.org/10.1016/j.asr.2015.10.006>.
- Meenal, R., Prawin Angel Michael, D. Pamela, Rajasekaran, E., 2021. Weather prediction using random forest machine learning model. *Indones. J. Electr. Eng. Comput. Sci.* 22 (2), 1208–1215. <https://doi.org/10.11591/ijeecs.v22.i2.pp1208-1215>.
- Meng, Xiaoyi, Gao, Xin, Sen, Li, Li, Shengyu, Lei, Jiaqiang, 2021. Monitoring desertification in Mongolia based on Landsat images and Google Earth engine from 1990 to 2020. *Ecol. Indic.* 129 <https://doi.org/10.1016/j.ecolind.2021.107908>.
- Midekisa, Alemayehu, Holl, Felix, Savory, David J., Andrade-Pacheco, Ricardo, Gething, Peter W., Bennett, Adam, Sturrock, Hugh J.W., 2017. Mapping land cover change over continental Africa using Landsat and Google Earth engine cloud computing. *PLoS One* 12 (9). <https://doi.org/10.1371/journal.pone.0184926>.
- Mohammed, Safwan, Al-Ebraheem, Ali, Holb, Imre J., Karam, Alsafadi, Dikkeh, Mohammad, Pham, Quoc Bao, Linh, Nguyen Thi Thuy, Szabo, Szilard, 2020. Soil management effects on soil water erosion and runoff in Central Syria-A comparative evaluation of general linear model and random forest regression. *Water* 12 (9). <https://doi.org/10.3390/w12092529>.
- Moiwo, Juana Paul, Lu, Wenxi, Tao, Fulu, 2012. GRACE, GLDAS and measured groundwater data products show water storage loss in western Jilin, China. *Water Sci. Technol.* 65 (9), 1606–1614. <https://doi.org/10.2166/wst.2012.053>.
- Naimi, Babak, Araújo, Miguel B., 2016. Sdm: a reproducible and extensible R platform for species distribution modelling. *Ecography* 39 (4), 368–375. <https://doi.org/10.1111/ecog.01881>.
- Naimi, Babak, Capinha, César, Ribeiro, Joana, Rahbek, Carsten, Diederik Strubbe, Reino, Luís, Miguel, B., Araújo, 2022. Potential for invasion of traded birds under climate and land-cover change. *Global Change Biol.* 28 (19), 5654–5666. <https://doi.org/10.1111/gcb.16310>.
- Park, Seonyoung, Jung, Im, Jang, Eunna, Rhee, Jinyoung, 2016. Drought assessment and monitoring through blending of multi-sensor indices using machine learning approaches for different climate regions. *Agric. For. Meteorol.* 216, 157–169. <https://doi.org/10.1016/j.agrformet.2015.10.011>.
- Pourghasemi, H.R., Moradi, H.R., Fatemi Aghda, S.M., 2013. Landslide susceptibility mapping by binary logistic regression, analytical hierarchy process, and statistical index models and assessment of their performances. *Nat. Hazards* 69 (1), 749–779. <https://doi.org/10.1007/s11069-013-0728-5>.
- Pravalié, Remus, 2021. Exploring the multiple land degradation pathways across the planet. *Earth Sci. Rev.* <https://doi.org/10.1016/j.earscirev.2021.103689>.
- Rahmati, Omid, Pourghasemi, Hamid Reza, Melesse, Assefa M., 2016. Application of GIS-based data driven random forest and maximum entropy models for groundwater potential mapping: a case study at mehran region, Iran. *Catena* 137, 360–372. <https://doi.org/10.1016/j.catena.2015.10.010>.
- Santos, Cassiano dos, Janaína, Lyra, Gustavo Bastos, Abreu, Marcel Carvalho, José Francisco de Oliveira-Júnior, Bohn, Leonardo, Cunha-Zeri, Gisleine, Zeri, Marcelo, 2022. Aridity indices to assess desertification susceptibility: a methodological approach using gridded climate data and cartographic modeling. *Nat. Hazards* 111 (3), 2531–2558. <https://doi.org/10.1007/s11069-021-05147-0>.
- “United Nations: convention to combat desertification in those countries experiencing serious drought and/or desertification, particularly in Africa.”. *Int. Leg. Mater.* 33 (5), 1994, 1328. <https://doi.org/10.1017/s0020782900026711>.
- Vapnik, Vladimir N., 1995. The nature of statistical learning theory. *Nat. Stat. Learn. Theory.* <https://doi.org/10.1007/978-1-4757-2440-0>.
- Wei, Haishuo, Wang, Juanle, Cheng, Kai, Ge, Li, Ochir, Altansukh, Davaasuren, Davaadorj, Chonokhuu, Sonomdagva, 2018. Desertification information extraction based on feature space combinations on the Mongolian plateau. *Rem. Sens.* 10 (10) <https://doi.org/10.3390/rs10101614>.
- Wei, Haishuo, Wang, Juanle, Han, Baomin, 2020. Desertification information extraction along the China-Mongolia railway supported by multisource feature space and geographical zoning modeling. *IEEE J. Sel. Top. Appl. Earth Obs. Rem. Sens.* 13, 392–402. <https://doi.org/10.1109/JSTARS.2019.2962830>.



- Wen, Ye, Guo, Bing, Zang, Wenqian, Ge, Dazhuan, Luo, Wei, Zhao, Huihui, 2020. Desertification detection model in naiman banner based on the albedo-modified soil adjusted vegetation index feature space using the Landsat8 OLI images. *Geomatics, Nat. Hazards Risk* 11 (1), 544–558. <https://doi.org/10.1080/19475705.2020.1734100>.
- Wulder, M.A., White, J.C., Cranny, M., Hall, R.J., Luther, J.E., Beaudoin, A., Goodenough, D.G., Dechka, J.A., 2008. Monitoring Canada's forests. Part 1: completion of the EOSD land cover project. *Can. J. Rem. Sens.* 34 (6).
- Xiao, J., Shen, Y., Tateishi, R., Bayaer, W., 2006. Development of topsoil grain size index for monitoring desertification in arid land using remote sensing. *Int. J. Rem. Sens.* 27 (12), 2411–2422. <https://doi.org/10.1080/01431160600554363>.
- Yang, X., Leys, J., 2014. Mapping wind erosion hazard in Australia using MODIS-derived ground cover, soil moisture and climate data. *IOP Conf. Ser.: Earth Environ. Sci.* vol. 17 <https://doi.org/10.1088/1755-1315/17/1/012275>.
- Yesilnacar, E., Topal, T., 2005. Landslide susceptibility mapping: a comparison of logistic regression and neural networks methods in a medium scale study, Hendek region (Turkey). *Eng. Geol.* 79 (3–4), 251–266. <https://doi.org/10.1016/j.enggeo.2005.02.002>.
- Zeng, Hongwei, Wu, Bingfang, Zhang, Miao, Zhang, Ning, Elnashar, Abdelrazek, Zhu, Liang, Zhu, Weiwei, Wu, Fangming, Yan, Nana, Liu, Wenjun, 2021. Dryland ecosystem dynamic change and its drivers in mediterranean region. *Curr. Opin. Environ. Sustain.* <https://doi.org/10.1016/j.cosust.2020.10.013>.